2024 European Control Conference (ECC)
June 25-28, 2024. Stockholm, Sweden

Design of distribution tariffs for energy hub networks to reduce carbon emissions

Varsha Behrunani, Federica Bellizio, Philipp Heer and John Lygeros

Abstract— **Utilizing demand-side flexibility provides a viable, cost-efficient and low-carbon alternative to standard grid reinforcement. Energy hubs can provide such a flexibility by leveraging both electrical and thermal grids. This work proposes a novel pricing model for distribution tariffs to fulfill network-wide objectives, while incentivising energy hubs to participate in a demand side flexibility scheme. In the first step, we formulate the optimization of the hub network and propose a novel approach to quantify the flexibility potential of the hubs. The energy hubs then provide the operator with their projected load and flexibility potential for the next day. Subsequently, the operator designs day-ahead tariffs to utilize this flexibility. The tariff incorporates the objectives of the network operator, reduction of carbon emissions in this study, while minimizing the energy costs. Finally, the energy hubs respond to the tariffs using a receding horizon controller to minimize the energy cost over the next day by exploiting building flexibility and both grids. An extensive numerical study on an network of 3 hubs with buildings of different sizes shows that the proposed pricing model can significantly reduce the carbon emissions with a low energy cost trade-off.**

I. Introduction

The stringent global decarbonization targets are driving a rapid integration of distributed energy resources (DERs) at low voltage levels. DERs can also provide flexibility to assist the system in accommodating more renewables while ensuring reliable operation [1]. In particular, energy hubs can leverage both electrical and thermal grids to enhance this flexibility provision and support the distribution system operators (DSOs) in fulfilling network-wide objectives, such as carbon emission reduction. This enables an improved utilization of the existing grid assets and a reduction of the investment costs to reinforce the network equipment [2].

DSOs are responsible for operation, control and maintenance of the distribution system to ensure security of supply. They procure energy from the wholesale market and sell it to end-users, setting the tariffs in accordance to the costs of various energy sources, grid upkeep, taxes, etc. DSOs can use these price signals to induce changes in the end-user's energy consumption, for example to reduce consumption during peak hours [6]. Energy hubs do not individually participate in energy service markets, but they generally respond to electricity distribution tariffs aiming to minimizing their energy costs. Therefore, when the distribution tariffs are designed to meet DER-specific objectives, the hubs indirectly perform demand response [3].

The design of distribution tariffs is a critical task and has been widely investigated in the literature. In [4], the authors identify ten different design criteria for efficient tariffs. While a highly granular tariff design would be more cost-reflective as it calculates the impact of individual customers on the grid cost, the higher granularity of the tariff would also result in a lower acceptability. Moreover, since all the energy hubs respond to the same price signal, this may lead to coordinated actions and result in high peak loads [5]. Dynamic tariffs have also recently been applied in practice by the Swiss DSO, Group E, to reduce the demand during peak hours [6].

Similarly, there has been extensive research into the operation of energy hubs that respond to distribution tariffs and fully exploit the link between hubs through peer-to-peer (P2P) energy trading to reduce energy costs. This can be achieved with either a centralized or a distributed approach. In the centralized approach, a central controller directly communicates with all hubs aiming to optimize multiple objectives [7], [8]. Here, the energy trading between the hubs can be modelled as a nonlinear power flow problem [9]. However, this requires information sharing and high computational effort, raising privacy and real-time infeasibility concerns. Conversely, distributed approaches can preserve the hubs' privacy, but may not be able to achieve a global optimum [10]. A centralized approach is used in this work.

Although the design of distributed tariffs and the optimal operation of energy hubs have been widely investigated individually, the integration of these two aspects remains a crucial research gap. This work proposes a novel pricing model for distribution tariffs which aims to address this gap. The strategy is centered on DSO pricing framework that accounts for the optimization of flexible energy hubs, and the communication between the DSO and the energy hubs. Network dynamics are neglected here as the formulation falls outside the scope of the price optimization. More specifically, we focus on building energy hubs as buildings account for a third of the global energy consumption and 40% of the total energy demand in Switzerland [20]. The key novelty of the proposed design is that it eliminates the need of the typically used carbon taxes or cap-and-trade programs as additional costs for the consumers to reduce the carbon emissions [19], as the carbon intensity is directly integrated into the electricity price. The design involves the following steps: 1) the energy hubs provides the operator with the projected load and the flexibility potential over the next 24 hours. 2) The operator designs the tariff to exploit this flexibility to meet its objectives. 3) A central receding horizon controller of the energy hubs responds to the tariff while minimizing the costs. An overview of the proposed strategy is presented in Fig. 1(a). The key contribution is

This research is supported by the SNSF through NCCR Automation (Grant Number 180545) and by the SWEET PATHFNDR project funded by the Swiss Federal Office of Energy SFOE (grant Nr. SI/502259-01).

V. Behrunani is with the Automatic Control Laboratory, ETH Zurich, Switzerland (email: bvarsha@ethz.ch) and the Urban Energy Systems Laboratory, Swiss Federal Institute of Material Science and Technology (Empa), Switzerland (email:varsha.behrunani@empa.ch).

F. Bellizio and P. Heer are with the Urban Energy Eystems Laboratory, Swiss Federal Institute of Material Science and Technology (Empa), Switzerland.(email: federica.bellizio@empa.ch, philipp.heer@empa.ch)

J. Lygeros is with the Automatic Control Laboratory, ETH Zurich, Switzerland (email: jlygeros@ethz.ch)

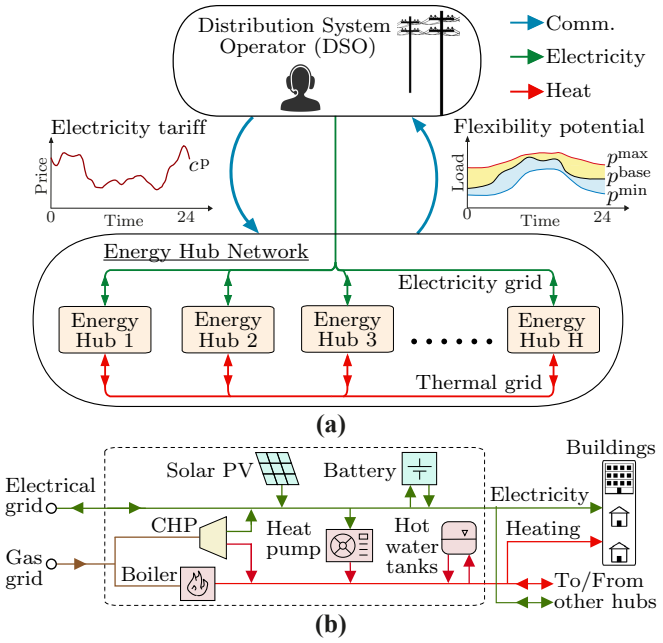

Fig. 1. (a) Overview of the physical connections between the distribution system and the energy hub network as well as the information flow between the DSO and the network controller under the proposed pricing scheme. (b) Topology of a single energy hub in the network [13].

twofold: i) A novel distribution tariff design for energy hubs that fulfills network-wide objectives, specifically carbon emission reduction in this work, while minimizing costs for each hub; ii) An analytical computation of the flexibility potential of the energy hubs for the following day.

The proposed design was tested via extensive numerical simulations on a 3-hub network, using realistic models of energy hubs and demand data. The performance was analysed in terms of the trade-off between carbon emission reduction and energy cost increase.

II. Model Description

We present the models used for the energy hub devices and the building thermal dynamics. The system comprises of a set of $\mathcal{H} = \{1, \dots, H\}$ interconnected energy hubs, and each energy hub supplies a set of buildings. Let $\mathcal{T} = \{0, \dots, T-1\}$ where T is the length of the horizon considered.

A. Energy Hub dynamics

Energy hub provides the interface between the buildings and the energy grids to serve the building electricity and heating demands. As shown in Fig. 1 (b), the energy hubs can include energy generation sources (e.g., photovoltaics) combined with different conversion and storage devices (e.g., battery, heat pump, etc.). Each hub is connected to the electricity and gas grid as well as to the local thermal grid. The hubs can trade electrical and thermal energy with other hubs via the electricity grid and the thermal grid, respectively.

Let $\mathcal{D}_n$ denote the set of devices controlled by the energy hub n. The dynamics of each energy hub device $i \in \mathcal{D}_n$ can be modelled as the following discrete time linear state space system that describes the evolution of its energy $\boldsymbol{x}_{t+1,i}$ [12]:

$$\left.\begin{aligned} \boldsymbol{x}_{t+1,i} &= A_i \boldsymbol{x}_{t,i} + B_i^{\mathrm{in}} \boldsymbol{u}_{t,i}^{\mathrm{in}} + B_i^{\mathrm{out}} \boldsymbol{u}_{t,i}^{\mathrm{out}} + D_i d_{t,i}, \\ \boldsymbol{x}_{t,i} &\in \mathcal{X}_{t,i},\ \boldsymbol{u}_{t,i}^{\mathrm{in}} \in \mathcal{U}_{t,i}^{\mathrm{in}},\ \boldsymbol{u}_{t,i}^{\mathrm{out}} \in \mathcal{U}_{t,i}^{\mathrm{out}}, \end{aligned}\right\} \forall t \in \mathcal{T} \tag{1}$$

where $d_{t,i}$ are the exogenous disturbances (e.g., solar radiation). Here, $\boldsymbol{u}_{t,i}^{\mathrm{in}}$ and $\boldsymbol{u}_{t,i}^{\mathrm{out}}$ are the inputs and outputs for device i, respectively, defined as

$$\boldsymbol{u}_{t,i}^{\mathrm{in}} = \begin{bmatrix} \boldsymbol{u}_{t,i}^{\mathrm{g,in}} \\ \boldsymbol{u}_{t,i}^{\mathrm{p,in}} \\ \boldsymbol{u}_{t,i}^{\mathrm{q,in}} \end{bmatrix} \quad \boldsymbol{u}_{t,i}^{\mathrm{out}} = \begin{bmatrix} \boldsymbol{u}_{t,i}^{\mathrm{p,out}} \\ \boldsymbol{u}_{t,i}^{\mathrm{q,out}} \end{bmatrix} \quad \forall t \in \mathcal{T}$$

where $\boldsymbol{u}_{t,i}^{\mathrm{g,in}}$, $\boldsymbol{u}_{t,i}^{\mathrm{p,in}}$ and $\boldsymbol{u}_{t,i}^{\mathrm{q,in}}$ are the gas, electricity and heating input to the device respectively, and $\boldsymbol{u}_{t,i}^{\mathrm{p,out}}$ and $\boldsymbol{u}_{t,i}^{\mathrm{q,out}}$ are the electricity and heating outputs from the device, respectively. For more details on how energy conversion and storage devices can be modelled in this framework, see [12].

There are three energy balancing constraints, one for each energy carrier (electricity, heating, gas). For hub n, the electricity energy balance constraint is

$$\begin{aligned} \boldsymbol{p}_{t,n}^{\mathrm{out}} + \sum_{i \in \mathcal{D}_n} \boldsymbol{u}_{t,i}^{\mathrm{p,out}} + \sum_{k \in \mathcal{H} \setminus \{n\}} \eta_{kn} \boldsymbol{p}_{t,kn}^{\mathrm{tr}} = \\ \boldsymbol{p}_{t,n}^{\mathrm{in}} + \sum_{i \in \mathcal{D}_n} \boldsymbol{u}_{t,i}^{\mathrm{p,in}} + \sum_{k \in \mathcal{H} \setminus \{n\}} \boldsymbol{p}_{t,nk}^{\mathrm{tr}} + L_{t,n}^{\mathrm{p}},\ \forall t \in \mathcal{T} \end{aligned} \tag{2a}$$

where $\boldsymbol{p}_{t,n}^{out} \geq 0$ and $\boldsymbol{p}_{t,n}^{in} \geq 0$ are the electricity purchased from and sold to the electricity grid, respectively, and $\boldsymbol{L}_{t,n}^{\mathrm{p}}$ is the total electricity demand of the buildings connected to the energy hub n at time step t. Here, $\boldsymbol{p}_{t,nk}^{\mathrm{tr}}$ is the energy traded and transferred from hub n to hub k at time step t. The total energy exported to all the hubs in the network from the hub n is $\sum_{k \in \mathcal{H} \setminus \{n\}} \boldsymbol{p}_{t,nk}^{\mathrm{tr}}$, while the energy imported from all the hubs in the network is $\sum_{k \in \mathcal{H} \setminus \{n\}} \eta_{kn} \boldsymbol{p}_{t,nk}^{\mathrm{tr}}$, where the efficiency η_{kn} takes into account the energy loss between the hubs. Similarly, the thermal energy balance constraint is

$$\begin{aligned} \sum_{i \in \mathcal{D}_n} \boldsymbol{u}_{t,i}^{\mathrm{q,out}} + \sum_{k \in \mathcal{H} \setminus \{n\}} \gamma_{kn} \boldsymbol{q}_{t,kn}^{\mathrm{tr}} = \\ \sum_{i \in \mathcal{D}_n} \boldsymbol{u}_{t,i}^{\mathrm{q,in}} + \sum_{k \in \mathcal{H} \setminus \{n\}} \boldsymbol{q}_{t,nk}^{\mathrm{tr}} + \boldsymbol{L}_{t,n}^{\mathrm{q}},\ \forall t \in \mathcal{T} \end{aligned} \tag{2b}$$

where $\boldsymbol{L}_{t,n}^{\mathrm{q}}$ is the total thermal demand of the buildings connected to the energy hub n at time step t and $\boldsymbol{q}_{t,nk}^{\mathrm{tr}}$ is the total thermal energy transferred from hub n to hub k at time step t. The total energy exported to all the hubs in the network from the hub n is $\sum_{k \in \mathcal{H} \setminus \{n\}} \boldsymbol{q}_{t,nk}^{\mathrm{tr}}$, while the energy imported from all the hubs in the network is $\sum_{k \in \mathcal{H} \setminus \{n\}} \gamma_{kn} \boldsymbol{q}_{t,nk}^{\mathrm{tr}}$, where the efficiency γ_{kn} takes into account the energy loss between the hubs. We assume that the efficiency is a function of the distance between the hubs and decreases linearly as the distance increases [18]. Finally, the gas energy balance constraint is given by

$$\boldsymbol{g}_{t,n}^{out} = \sum_{i \in \mathcal{D}_n} \boldsymbol{u}_{t,i}^{\mathrm{g,in}}, \quad \forall t \in \mathcal{T} \tag{2c}$$

Finally, we introduce a constraint that limits the electrical and thermal energy traded between hubs,

$$\left.\begin{aligned} 0 \leq \boldsymbol{p}_{t,nk}^{\mathrm{tr}} \leq \kappa_{nk}^{\mathrm{p}}, \\ 0 \leq \boldsymbol{q}_{t,nk}^{\mathrm{tr}} \leq \kappa_{nk}^{\mathrm{q}}. \end{aligned}\right\} \forall k \in \mathcal{H}_{\setminus \{n\}}, \forall t \in \mathcal{T} \tag{3}$$

Setting the limit κ_{nk}^{p} and κ_{nk}^{q} on the energy that can be traded between the hubs n and k to zero can also be used to define specific trading network topologies and specify if two hubs are not connected or cannot trade with one another.

B. Building Dynamics

Let $\mathcal{B}_n$ denote the set of buildings that are supplied by energy hub n. Following [11], the thermal dynamics of the building $j \in \mathcal{B}_n$ at time $t \in \mathcal{T}$ are modelled through a simplified state space model:

$$\left.\begin{aligned} \boldsymbol{x}_{t+1,j} &= A_j \boldsymbol{x}_{t,j} + B_j \boldsymbol{u}_{t,j} + D_j \boldsymbol{d}_{t,j} \\ \boldsymbol{y}_{t,j} &= C_j \boldsymbol{x}_{t,j} \end{aligned}\right\} \forall t \in \mathcal{T} \quad (4a)$$

where $\boldsymbol{x}_{t,j}$ are the states representing the temperatures of the individual zones and may include the temperature of walls, floors and ceiling layers of the building, $\boldsymbol{y}_{t,j}$ are the measured outputs (e.g., room temperatures, humidity), $\boldsymbol{u}_{t,j}$ are the controllable inputs and activation units (e.g., radiators, air handling units), and $d_{t,j}$ are the disturbances that affect the building (e.g., ambient temperature, solar radiation or internal gains). Here, the state space matrices A_j, B_j, D_j, and C_j capture the building characteristics. In this work, the measured outputs are the temperatures of all the zones in the building. This is achieved by designing C_j to select only the zone temperatures states from the state vector $\boldsymbol{x}_{t,j}$. We also assume that the building management system has access to perfect forecasts for the disturbances and the electrical demand. While this assumption is unrealistic in practice, it can easily be relaxed by introducing forecast uncertainty and feedback policies [12][13]. Furthermore, the building models are assumed to be linear as they only consider radiant heating systems and do not have air-handling units (AHUs) in accordance to buildings in Europe.

A number of constraints are introduced to model occupant comfort and device limitations. Equation (4b) ensures that the room temperatures stay within the time varying comfort bounds and equation (4c) enforces the physical constraints on the inputs to the building.

$$\boldsymbol{T}_{\mathrm{r},t}^{\min} \leq \boldsymbol{y}_{t,j} \leq \boldsymbol{T}_{\mathrm{r},t}^{\max}, \quad \forall t \in \mathcal{T} \quad (4b)$$

$$\boldsymbol{u}_{j}^{\min} \leq \boldsymbol{u}_{t,j} \leq \boldsymbol{u}_{j}^{\max}, \quad \forall t \in \mathcal{T} \quad (4c)$$

where $\boldsymbol{u}_j^{\min}$ and $\boldsymbol{u}_j^{\max}$ are the minimum and maximum limits of the inputs respectively. We limit attention to commercial buildings and set the minimum temperature, $\boldsymbol{T}_{\mathrm{r},t}^{\min}$, and maximum temperature, $\boldsymbol{T}_{\mathrm{r},t}^{\max}$, to 18°C and 26°C respectively between 22:00 and 6:00, and 21°C and 23°C otherwise.

Each building j has its own electrical and thermal demand at each time step t, $\boldsymbol{l}_{t,j}^{\mathrm{p}}$ and $\boldsymbol{l}_{t,j}^{\mathrm{q}}$, respectively. The total electrical and thermal energy demand of the buildings connected to energy hub n at time t is defined by

$$\boldsymbol{L}_{t,n}^{\mathrm{p}} = \sum_{j \in \mathcal{B}_n} \boldsymbol{l}_{t,j}^{\mathrm{p}} \ , \quad \boldsymbol{L}_{t,n}^{\mathrm{q}} = \sum_{j \in \mathcal{B}_n} \underbrace{e_j^{\mathrm{T}} \boldsymbol{u}_{t,j}}_{:=\boldsymbol{l}_{t,j}^{\mathrm{q}}} , \quad \forall t \in \mathcal{T} \quad (5)$$

where $\boldsymbol{e}_j$ selects the inputs from $\boldsymbol{u}_{t,j}$ corresponding to the thermal inputs to the radiators of the building.

Finally, the full constraint set for each energy hub n with devices $\mathcal{D}_n$ and buildings $\mathcal{B}_n$ is:

$$\mathrm{EH}_n := \left\{ \begin{array}{l} \left\{ \boldsymbol{p}_{t,n}^{\mathrm{in}},\ \boldsymbol{p}_{t,n}^{\mathrm{out}},\ \boldsymbol{L}_{t,n}^{\mathrm{p}},\ \boldsymbol{L}_{t,n}^{\mathrm{q}},\ \boldsymbol{p}_{t,nk}^{\mathrm{tr}},\ \boldsymbol{q}_{t,nk}^{\mathrm{tr}} \right\}_{t \in \mathcal{T}} : \\ \exists \left\{ \boldsymbol{u}_{t,i}^{\mathrm{in}}, \boldsymbol{u}_{t,i}^{\mathrm{out}} \right\}_{t \in \mathcal{T}} \text{ s.t. (1, 2, 3) hold } \forall i \in \mathcal{D}_n \\ \exists \left\{ \boldsymbol{u}_{t,j} \right\}_{t \in \mathcal{T}} \text{ s.t. (4, 5) hold } \forall j \in \mathcal{B}_n \end{array} \right\}$$

Note that the network dynamics are neglected here as the formulation falls outside the scope of the price optimization.

III. Optimization and Flexibility Quantification

The optimal operation of the energy hubs aims to minimize the costs of purchasing electricity and gas from the grid, over a finite horizon, while satisfying the comfort and operational constraints in the system. The joint operation of the hubs allows them to engage in P2P trading, resulting in increased self-reliance, flexibility and utilisation of renewable generation and storage resources. We assume that the cost of electricity and gas at time t, $\boldsymbol{c}_t^{\mathrm{p}}$ and $\boldsymbol{c}_t^{\mathrm{g}}$ respectively, is known by the hub controller for the complete horizon $\mathcal{T}$. The energy hubs can also feed excess electricity into the grid with a known constant feed-in tariff $\boldsymbol{c}_t^{\mathrm{f}}$ at time t. Furthermore, the grid operator imposes an additional tariff, $\boldsymbol{c}_{tr}^{\mathrm{f}}$, on the hubs for the use of the electricity grid infrastructure, e.g. for bilateral trades between them. The resulting optimization of the energy hubs can be formulated as

$$\begin{aligned} \min \sum_{t=0}^{T-1} \left(\sum_{n=1}^{H} \left(\begin{array}{r} \boldsymbol{g}_{t,n}^{\mathrm{out}} \cdot \boldsymbol{c}_t^{\mathrm{g}} + \boldsymbol{p}_{t,n}^{\mathrm{out}} \cdot \boldsymbol{c}_t^{\mathrm{p}} - \boldsymbol{p}_{t,n}^{\mathrm{in}} \cdot \boldsymbol{c}_t^{\mathrm{f}} \\ + \textstyle\sum_{k \in \mathcal{H} \setminus \{n\}} \boldsymbol{p}_{t,nk}^{\mathrm{tr}} \cdot \boldsymbol{c}_t^{\mathrm{tr}} \end{array} \right) \right) \\ \text{s.t.} \left\{ \boldsymbol{p}_{t,n}^{\mathrm{in}}, \boldsymbol{p}_{t,n}^{\mathrm{out}}, \boldsymbol{L}_{t,n}^{\mathrm{p}}, \boldsymbol{L}_{t,n}^{\mathrm{q}}, \boldsymbol{p}_{t,nk}^{\mathrm{tr}}, \boldsymbol{q}_{t,nk}^{\mathrm{tr}} \right\}_{t \in \mathcal{T}} \in \mathrm{EH}_n, \quad \forall n \in \mathcal{H} \end{aligned} \quad (6)$$

The centralised controller solves the optimal control problem to compute the dispatch of all the devices in each of the hubs, as well as the energy traded between hubs, using an MPC strategy. At each time-step, the optimization determines the optimal control inputs for the system over the full horizon $\mathcal{T}$, and applies only the first of these inputs to the system. The process is then repeated at the next time step. The receding horizon implementation brings feedback into the process and allows the controller to continuously adapt to new measurements, forecast information, and suppress the effect of disturbances. Distributed control algorithms, such as the strategy proposed in [10] based on consensus version of ADMM, can be used to solve this problem, achieving the optimal operation of the hubs, while mitigating concerns over privacy and scalability. To ensure feasibility of the optimization, an additional slack variable σ_t is added to the comfort bounds in (4b) and the violation of the comfort constraints is penalised in the cost function by adding a term with this slack variable multiplied with a high penalty.

A. Quantifying the flexibility potential of energy hubs

One of the key factors affecting the optimal dispatch of the hubs and the energy imported from the grid is the electricity tariff, $\boldsymbol{c}_t^{\mathrm{p}}$, which drives the flexibility provision from the different flexible devices in the buildings, including schedulable loads such as washing machines and dishwashers, and storage devices such as batteries and thermal storage tanks.

The flexibility that an energy hub provides for a set of buildings, can be represented as an envelope and quantified by computing the maximum and minimum energy demand of the system over a horizon, within which the occupant's comfort and the operational constraints are satisfied [14]. The baseline load of the system, which is the energy demand of a reference case that represents the power usage in a locally optimal situation, lies within such a consumption range. Fig. 2 illustrates the adopted definition of flexibility. The black line is the baseline load. The blue line is the minimum load

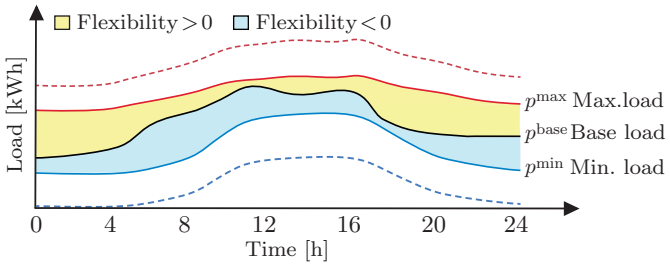

Fig. 2. Schematic of the flexibility potential of an energy hub. The solid lines show the nominal flexibility of the hub. The dotted lines show the potential flexibility of the same hub with the use of a storage device.

of the building and the blue area is the negative flexibility provided by decreasing power consumption below the baseline. Conversely, the red line is the maximum load and the yellow area represents the positive flexibility provided by increasing the power demand.

The presence of storage devices in the energy hub can significantly increase the flexibility potential of the system. However, this makes the quantification of the flexibility potential more challenging. The amount of flexible energy provided by the storage devices and how long it can be provided for depends on the current state of charge (SoC), the charging/discharging behaviours in the previous time step, the power rating and the capacity of the installed storage device. The dotted lines in Fig. 2 shows the flexibility potential with the addition of a battery. If the battery is sufficiently charged, the negative flexibility increases at the next time instance as the battery may supply part of the electrical energy load, decreasing the consumption from the grid. Additionally, as long as the battery is not at maximum capacity, it can still be charged increasing consumption from the grid. Therefore, a fixed maximum and minimum load would depend on when the battery is charged or discharged.

More precisely, in this study, we describe the flexibility potential of energy hubs including storage devices for a horizon of T hours using (a) the nominal flexibility when no electrical or thermal storage devices are considered, and (b) the capacity s^{cap} and the SoC of the installed storage devices at midnight. The information (b) allows the DSO to track the dynamics of the storage devices over the horizon to exploit the flexibility they can provide while ensuring a feasible operation. The nominal flexibility for the energy hubs is quantified by computing the fixed baseline, maximum and minimum energy demand, as described below:

- Minimum load curve ($p^{\min}$): Solve Eq. (6) using constant $\boldsymbol{c}_t^{\text{p}} = \boldsymbol{c}^{\text{p}} \geq \boldsymbol{c}_t^{\text{f}}$ and excluding storage devices.
- Baseline load curve (p^{base}): Solve Eq. (6) to achieve a reference temperature of 22°C (Eq. (4b)) using constant $\boldsymbol{c}_t^{\text{p}} = \boldsymbol{c}^{\text{p}} \geq \boldsymbol{c}_t^{\text{f}}$ and excluding storage devices.
- Maximum load curve ($p^{\max}$): Solve Eq. (6) to maximize energy usage using constant negative $\boldsymbol{c}_t^{\text{p}} = \boldsymbol{c}^{\text{p}}$ and $\boldsymbol{c}_t^{\text{f}}$ and excluding storage devices where $\boldsymbol{c}^{\text{p}}, \boldsymbol{c}_t^{\text{f}} \leq 0$.

The dynamics of the storage system are modelled using a state space system which describes the evolution of SoC x_t^{s}:

$$\left.\begin{aligned} \boldsymbol{x}_{t+1}^{\text{s}} &= A^{\text{s}}\boldsymbol{x}_t^{\text{s}} + B^{\text{u}}\boldsymbol{u}_t^{\text{u}} - B^{\text{d}}\boldsymbol{u}_t^{\text{d}}, \\ \boldsymbol{x}_t^{\text{s}} &\in \left[s^{\min}, s^{\max}\right], \quad x_0^{\text{s}} = s_0 \\ \boldsymbol{u}_t^{\text{u}} &\in \left[0, u^{\max} \cdot z_t\right], \\ \boldsymbol{u}_t^{\text{d}} &\in \left[0, u^{\max} \cdot (1 - z_t)\right], \quad z_t \in \{0,1\} \end{aligned}\right\} \forall t \in \mathcal{T} \quad (7)$$

where s_0 is the initial SoC, $s^{\min}$ and $s^{\max}$ are the minimum and maximum storage levels, u_t^{u} and u_t^{d} are the charged and discharged, respectively, and $u^{\max}$ is the maximum rate at which the storage can be charged or discharged energy. The binary value z_t ensures that the storage is not simultaneously charged and discharged.

Finally, the full constraint set to describe the flexibility potential of the energy hub network is

$$\text{FL} := \left\{ \begin{aligned} &\left\{p_t^{\text{proj}}\right\}_{t\in\mathcal{T}} : \exists \left\{\boldsymbol{u}_t^{\text{u}}, \boldsymbol{u}_t^{\text{d}}, \boldsymbol{z}_t\right\}_{t\in\mathcal{T}} \text{ such that} \\ &\sum_{t=0}^{T-1} p_t^{\text{proj}} = \sum_{t=0}^{T-1} p_t^{\text{base}} \\ &p_t^{\min} - u_t^{\text{d}} \leq p_t^{\text{proj}} \leq p_t^{\max} + u_t^{\text{u}}, \ \forall t \in \mathcal{T}, \\ &u_t^{\text{d}} \leq p_t^{\min}, \quad \forall t \in \mathcal{T}, \text{ and (7) hold} \end{aligned} \right\}$$

where p^{proj} is the projected load of the energy hubs. The first constraint ensures that the total load still satisfies the nominal demand over the complete horizon. This constraint ensures that the projected load does not stick to the minimum load when the energy cost is minimised, resulting in a negative flexibility for the entire following day, thereby ensuring a more realistic load shift scenario. The second constraint ensures that the load does not exceed the flexibility bounds at any given time. The flexibility bounds, in particular, are time varying depending on the current SoC of the installed storage devices. Finally, the last constraint ensures non-negativity of the lower bound.

IV. Distribution Tariff Pricing Model

The objective of the distribution tariffs is to fulfil network-wide objectives (here, carbon emission reduction) while reducing the energy cost of the hubs. A naive approach is to model the prices so that these two objectives are balanced. Let $\alpha \in [0,1]$ be a tuning parameter that enables the DSO to set its priority and trade-off the two objectives, and consider an electricity price given by

$$c_t^{\text{p}} = \left(\alpha \cdot c_t^{\text{n.carbon}} + (1-\alpha) \cdot c_t^{\text{n.cost}}\right), \quad \forall t \in \mathcal{T}$$

where $c_t^{\text{n.cost}}$ and $c_t^{\text{n.carbon}}$ are the normalised cost of energy and the normalised carbon intensity of electricity at time t, respectively. While this strategy results in prices that reflect the desired objective, the prices could be too high or too low with respect to the actual energy costs. High prices result in overcharging the energy hubs for their basic energy usage, whereas low prices are insufficient in recovering the DSO's cost of procuring energy from the wholesale market resulting in a loss. Hence, it is important to scale the price curve in a suitable manner in line with expected costs of the system.

In the proposed pricing model for distribution tariffs, the true cost of the system is computed by taking into account the demand and the flexibility potential of the energy hub network. At midnight, the energy hubs compute their flexibility for the following day and communicate $p^{\min}$, p^{base} and $p^{\max}$ to the DSO. Subsequently, the DSO can compute the projected load of the hubs, p^{proj}, assuming that the SoC of all the energy hubs' storage devices is 50% at the start of the day, i.e. $s_0 = 0.5 \cdot s^{\text{cap}}$. This is viable as it is assumed that the DSO has access to information

about the installed capacity and operating limits of the storages. This assumption is not unreasonable; for example, this information must be communicated upon installation under the current Swiss regulations [17]. The projected load is computed by solving the following optimization under the desired prices:

$$\begin{aligned} \min \quad & \sum_{t=0}^{T-1} \left(\alpha \cdot c_t^{\text{n.carbon}} + (1-\alpha) \cdot c_t^{\text{n.cost}}\right) \cdot p_t^{\text{proj}} \\ \text{s.t.} \quad & \left\{p_t^{\text{proj}}\right\}_{t\in\mathcal{T}} \in \text{FL} \end{aligned} \tag{8}$$

This is a multi-objective optimization wherein the cost function balances the cost of energy and carbon intensity of electricity based on the parameter α. The optimization minimizes the cost of the hubs with the desired price curve while ensuring that the projected load is within the flexibility potential of the hubs. As a result, the computed projected load provides a good estimate of the future load shifting of the energy hubs. The distribution tariffs are finally given by:

$$\boldsymbol{c}_t^{\text{p}} = \text{R} \cdot \left(\alpha \cdot c_t^{\text{n.carbon}} + (1-\alpha) \cdot c_t^{\text{n.cost}}\right), \quad \forall t \in \mathcal{T} \tag{9}$$

where R is a scaling factor calculated as the ratio of the true energy costs incurred by the network operator (without normalization) to the total costs obtained using the desired prices:

$$\text{R} = \frac{\sum_{t=0}^{T-1} \left(c_t^{\text{cost}}\right) \cdot p_t^{\text{proj}}}{\sum_{t=0}^{T-1} \left(\alpha \cdot c_t^{\text{n.carbon}} + (1-\alpha) \cdot c_t^{\text{n.cost}}\right) \cdot p_t^{\text{proj}}} \tag{10}$$

The designed tariffs are used by the energy hub networks to compute the optimal control inputs over the next 24h by solving (6) at every time step. The process is repeated at the beginning of each day. Hence, the optimization of the energy hubs is completely decoupled from the DSO and the hubs communicate their flexibility once every day and receive the prices from the DSO for the following day. Fig. 1(a) illustrates the resulting process and the information structure. The described pricing model can be used in a similar manner for various network-wide objectives, not limited to two.

While the optimal dispatch problem of the energy hubs can be solved in a distributed manner to handle scalability concerns [10], the price optimization is solved centrally for a single DSO using the information communicated by all the hubs. This involves a limited number of decision variables and constraints and needs to be solved only once every day.

V. Numerical Study

We illustrate the proposed pricing model for distribution tariffs on an energy hub network comprising three energy hubs, each connected to a set of buildings. The energy hubs and buildings were designed using the energy hub modelling toolbox [15]. Hub 1 comprises solar PV, battery energy storage, and a heat pump, Hub 2 comprises solar PV, battery energy storage, a hot water storage tank and a heat pump, and Hub 3 consists of a heat pump. The electricity demand profiles of hubs are based on buildings located at the ETH Zürich and Empa Dübendorf campuses in Switzerland. We consider three sources of disturbances for the buildings: ambient temperatures, solar radiation, and building internal gains. The data for environmental disturbances were taken from [13] for the city of Zürich and historical data was used for the building internal gains. Data from [16] was used for the cost of energy and the carbon intensity. The feed-in tariff used was 0.12 CHF/kWh; note that no gas devices were considered in this study. The performance of the proposed strategy was evaluated for a simulation period of one week in January 2018. The optimization was solved with a horizon $T = 24$h with a sampling resolution of 1h.

Fig. 3 shows the nominal flexibility potential of the network for a selected day (24h) within the whole simulation period. The flexibility potential is higher at the beginning and end of the day due to the wider temperature bounds. Less heating is required to maintain the minimum temperature and the higher upper temperature bound increases the positive flexibility. During the day, the flexibility potential is much narrower due to tighter comfort bounds and increased impact of disturbances, such as solar radiation.

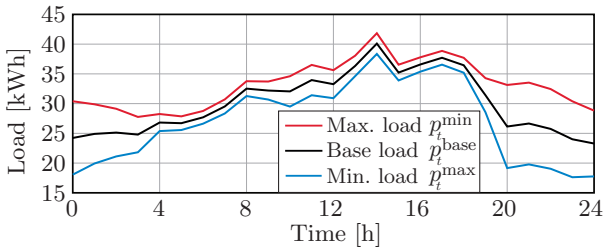

Fig. 3. Nominal flexibility potential of the energy hub network for 24h.

In Fig. 4 (a), the hourly cost of procuring electricity, c_t^{cost}, and the hourly carbon intensity of the grid, c_t^{carbon}, are compared to the electricity distribution tariff, c_t^{p}, computed using two α values for a period of 24h within the whole simulation period. A lower $\alpha = 0.3$ resulted in a tariff that is similar to the electricity prices as the DSO prioritizes energy cost more than the carbon intensity. Conversely, $\alpha = 0.8$ resulted in a tariff with a similar trend to the carbon intensity prices, as the DSO's main goal is to reduce carbon emissions. Fig. 4(b) shows the resulting shift in the imported energy from the grid for different α values in response to the change in the tariff. For each α, the energy demand was higher when the price was low and decreased when the price peaked.

Fig. 5 illustrates the trade-off between the total carbon emissions and total cost of the energy hubs for different α values for the whole simulation period of 7 days. As α increased, the carbon emissions decreased drastically and saturated for $\alpha = 0.6$, beyond which no further decrease was observed. Varying the value of α also resulted in a cost increase; note, however that the cost increase is significantly smaller than the decrease in emissions as a percentage . For $\alpha = 0.6$, the carbon emissions were reduced by 25%, with a slight cost increase of 3.5%. Similarly, for $\alpha = 1$, the emissions decreased by 25% with a corresponding cost increase of 7%. This suggests that the proposed pricing model can help the DSO acheive network-wide objectives without impacting the energy cost. The same trend was also observed using different energy hub configurations, buildings sizes and simulation data.

Finally, Table I compares the total energy cost and carbon emissions both with and without P2P electrical and thermal energy trading between the hubs for different α values. P2P trading result in a lower cost and lower carbon emissions for

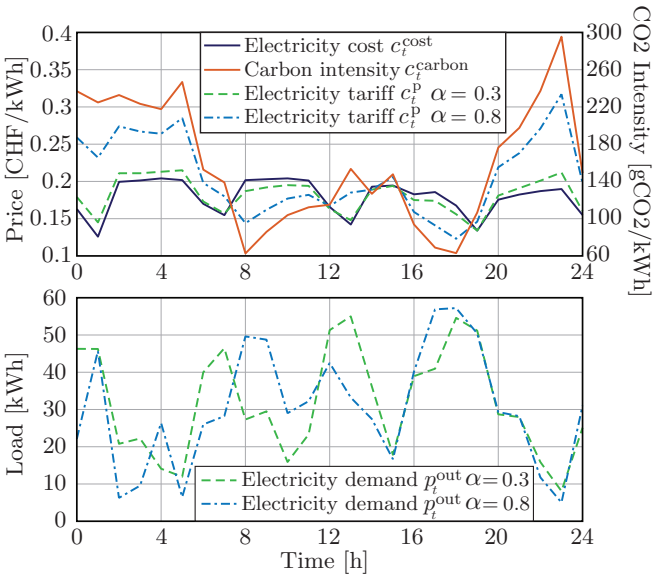

Fig. 4. Results of the proposed strategy for over 24 h using $\alpha = 0.3$ and $\alpha = 0.8$: (a) Energy tariff computed compared to the original energy cost and the carbon intensity of electricity and (b) the resulting electricity demanded from the grid.

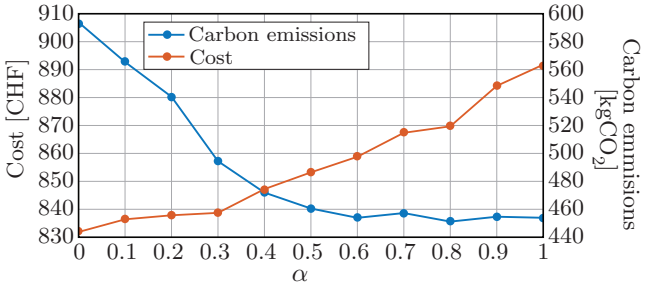

Fig. 5. Total carbon emissions and energy cost of the hub network over a simulation period of 1 week for different values of α.

all α values by exploit P2P trading to share resources. In the absence of bilateral trading, the cost and carbon emissions still follow the same trend for different α values.

	With P2P Trading				**Without P2P Trading**			
α	0	0.3	0.8	1	0	0.3	0.8	1
Total Cost (CHF)	832	841	869	891	849	857	884	904
Total Emissions (kgCO$_2$)	595	495	454	455	603	530	501	496

TABLE I

TOTAL EMISSIONS AND ENERGY COST OF THE HUB NETWORK OVER THE WHOLE SIMULATION PERIOD FOR DIFFERENT α.

VI. CONCLUSION

Electricity distribution tariffs play a major role in determining the energy demand and the optimal dispatch of energy hubs. A novel pricing model was proposed for the design of distribution tariffs based on the desired network-wide objectives, such as reduction of the grid carbon emissions, while minimizing the cost of the energy hubs. The approach relies on the analytical computation of the flexibility potential of energy hubs for the following day. Numerical simulations on a three-hub network demonstrates the price design mechanism with different DSO's priorities by varying the parameter α. By choosing a reasonably high α, the carbon emission of the hubs was significantly reduced with a negligible cost increase. This is achieved by leveraging building flexibility and bilateral trading using both the electrical and thermal grid to shift the energy demand in response to the prices. Future work aims to extend the proposed framework to a distributed setting and other sectors beyond buildings, test the strategy with an increasing number of hubs and under different hub topologies, and finally compare it to existing state-of-the-art approaches.

ACKNOWLEDGMENT

The authors would like to thank Dr. Hanmin Cai for his insightful comments during this work.

REFERENCES

[1] D. Božič and M. Pantoš, "Impact of electric-drive vehicles on power system reliability," Energy, vol. 83, pp. 511–520, 2015.
[2] G. Strbac D. Pudjianto, M. Aunedi, P. Djapic, F. Teng, X. Zhang, H. Ameli, R. Moreira, and N. Brandon, "Role and value of flexibility in facilitating cost-effective energy system decarbonisation," Progress in Energy, vol. 2, no. 4, p. 042001, 2020.
[3] F. Brahman, M. Honarmand and S. Jadid, "Optimal electrical and thermal energy management of a residential energy hub, integrating demand response and energy storage system," Energy and Buildings 90, pp.65-75, 2015.
[4] C. Winzer, "Conceptual Recommendations for Optimal Grid Tariff Design," Available at SSRN 4484167, 2023.
[5] R. A. Verzijlbergh, L. J. De Vries and Z. Lukszo, "Renewable energy sources and responsive demand. Do we need congestion management in the distribution grid?," IEEE Transactions on Power Systems, vol. 29, no. 5, pp. 2119–2128, 2014.
[6] Dynamische tarife für ein effizientes stromsystem | VSE. [Online]. Available: https://www.strom.ch/de/nachrichten/dynamische-tarife-fuer-ein-effizientes-stromsystem.
[7] R. Smith, V. Behrunani and J. Lygeros, "Control methods for multi-carrier energy systems from the building to the network scale," Annual Review of Control, Robotics, and Autonomous Systems, vol. 5, 2022.
[8] A. Maroufmashat, A. Elkamel, M. Fowler, S. Sattari, R. Roshandel, A. Hajimiragha, S. Walker and E. Entchev, "Modeling and optimization of a network of energy hubs to improve economic and emission considerations," Energy, vol. 93, pp. 2546–2558, 2015.
[9] M. Geidl and G. Andersson, "Optimal power flow of multiple energy carriers," IEEE Transactions on Power Systems, vol. 22, pp. 145–155, 2007.
[10] V. Behrunani, H. Cai, P. Heer, R.S. Smith and J. Lygeros, "Distributed Multi-Horizon Model Predictive Control for Network of Energy Hubs," Control Engineering Practice (accepted), 2024. *arXiv preprint arXiv:2304.14089*.
[11] G. Darivianakis, A. Georghiou, R.S. Smith and J. Lygeros, "The Power of Diversity: Data-Driven Robust Predictive Control for Energy-Efficient Buildings and Districts," IEEE Transactions on Control Systems Technology, vol. 27, no. 1, pp. 132-145, 2019.
[12] G. Darivianakis, A. Georghiou, R.S. Smith and J. Lygeros, "A stochastic optimization approach to cooperative building energy management via an energy hub," IEEE Conference on Decision and Control (CDC), vol. 54, pp. 7814-7819, 2015.
[13] V. Behrunani, F. Micheli, J. Mehr, P. Heer and J. Lygeros, "Stochastic MPC for energy hubs using data driven demand forecasting," IFAC World Congress, vol. 56, no. 2, pp. 11026-11031, 2023.
[14] C. Yongbao, X. Peng, G. Jiefan, S. Ferdinand and L. Weilin, "Measures to improve energy demand flexibility in buildings for demand response (DR): A review," Energy and Buildings, vol. 177, pp. 132-145, 2018.
[15] G. Darivianakis, A. Georghiou, R. S. Smith and J. Lygeros, EHCM Toolbox, ETH Zürich Automatic Control Laboratory, 2015.
[16] M. Rüdisüli, E. Romano, S. Eggimann and M. K. Patel, "Decarbonization strategies for Switzerland considering embedded greenhouse gas emissions in electricity imports," Energy Policy, vol. 162, 2022.
[17] Werkvorschriften CH (WV-CH), Verband Schweizerischer Elektrizitätsunternehmen VSE, 2021.
[18] S. Klyapovskiy, S. You, H. Cai and H. W. Bindner, "Incorporate flexibility in distribution grid planning through a framework solution," International Journal of Electrical Power & Energy Systems, vol. 111, pp. 66-78, 2019.
[19] J. Carl, D. Fedor, "Tracking global carbon revenues: A survey of carbon taxes versus cap-and-trade in the real world," Energy Policy, vol. 96, pp. 50-77, 2016.
[20] S. Cozza, J. Chambers, M. K. Patel, "Measuring the thermal energy performance gap of labelled residential buildings in Switzerland," Energy Policy, vol. 137, 2020.